



	<b>Experiment title:</b> A XAFS spectroscopy study of local environment around gold in high T/P aqueous sulfide and chloride solutions: Implications for the mechanisms of gold deposits formation	<b>Experiment number:</b> 30 02 720
<b>Beamline:</b> BM30B	<b>Date of experiment:</b> from: 7 Jun 2005 to: 13 Jun 2005	<b>Date of report:</b> 8 September 2005
<b>Shifts:</b> 18	<b>Local contact(s):</b> Jean-Louis Hazemann, BM30B (FAME), ESRF	<i>Received at ESRF:</i>
<b>Names and affiliations of applicants</b> (* indicates experimentalists): * <b>Boris Tagirov</b> , ETH, Zurich, Switzerland * <b>Jean-Louis Hazemann</b> & * <b>Olivier Proux</b> , Laboratoire de Cristallographie, ESRF-CNRS, Grenoble * <b>Jacques Schott</b> & * <b>Gleb Pokrovski</b> , Laboratoire des Mécanismes & Transferts en Géologie, LMTG, Toulouse		

### Report:

**Experimental.** The dissolution and atomic structure of gold in chloride and sulfide aqueous solutions were examined by XAFS spectroscopy at Au L<sub>3</sub>-edge at temperatures from 200 to 450°C and pressures to 600 bar, using an X-ray cell recently developed at the Laboratoire de Cristallographie<sup>1</sup>. This cell allows simultaneous measurement of the absolute concentration of the absorbing element in the fluid (from edge-step height in transmission mode, fluid density and absorption cross-section of the element), and atomic environment around the absorber (from analysis of XANES and EXAFS spectra in fluorescence and/or transmission mode)<sup>2</sup>. An improved internal cell design used in the present experiment utilizes two mobile pistons equipped with Viton joints and inserted into a glassy-carbon tube with low absorption coefficient for X-rays. This construction has already been successfully applied in our recent Sb XAFS study to 500°C<sup>3</sup>.

**Results from the chloride system.** Two experiments were performed in the system 0.035m HAu<sup>(III)</sup>Cl<sub>4</sub>-0.5m NaCl-0.01m HCl ± Au(metal) at 600 bar as a function of temperature and time. It was found that below 100°C, the XAFS spectra are consistent with the plane-square Au<sup>(III)</sup>Cl<sub>4</sub><sup>-</sup> complex reported in previous low-temperature XAFS and Raman studies<sup>4,5</sup>. At higher temperature, there is a fast decrease of Au concentration accompanied by the reduction of Au(III) to metallic gold. This behavior is also observed in our previous experiment on the same system using a sapphire cell. Batch-reactor solubility studies indicate, however, that above 200°C, AuCl<sub>4</sub><sup>-</sup> in the presence of metallic gold should convert to AuCl<sub>2</sub><sup>-</sup> and attain concentrations 10 times higher than measured in our experiments<sup>6</sup>. This discrepancy might be attributed to a reaction of Au(III) with the carbon cell walls. Another possibility could be the beam-induced reduction of AuCl<sub>2</sub><sup>-</sup> into Au<sup>0</sup> (e.g., ref. 4).

**Results from the sulfur system.** Four experiments were performed in NaOH solutions, one in pure water, and one in the presence of H<sub>2</sub>SO<sub>4</sub> by allowing a foil of metallic gold and a desired mass of sulfur crystals to react with corresponding solutions at high temperature. Dissolved sulfur concentrations ranged from 0.1 to 4 mol/kg. As show thermodynamic equilibrium calculations<sup>7</sup>, at neutral to basic pH (4-8), the reaction of sulfur with NaOH-H<sub>2</sub>O above 200°C produces sulfide (H<sub>2</sub>S, HS<sup>-</sup>) and sulfate (NaSO<sub>4</sub><sup>-</sup>, HSO<sub>4</sub><sup>-</sup>, SO<sub>4</sub><sup>2-</sup>) species. At acid pH (<3) above 300-400°C, however, SO<sub>2</sub> becomes the dominant species. In all experiments below 400°C, dissolved Au concentrations derived from the absorption edge jump attain a steady state within a few hours (Fig. A & B). The dissolved sulfur concentrations, estimated from the before-edge absorption in transmission mode (sulfur is the major contributor to the absorption below the Au L<sub>3</sub> edge in our solutions), are in agreement with predicted sulfur solubilities within better than 30% of the value. In some S-rich experiments at 400 and 450°C, a drop of dissolved sulfur and gold concentrations with time was observed. This is likely due to precipitation of some amount of sulfur in colder parts of the cell close to the Viton rings and fluorescence window.

Steady-state Au contents measured in our experiments in the system S-NaOH at neutral pH in a wide range of S concentrations are in excellent agreement (within 0.2 log units) with the predicted equilibrium concentrations using the thermodynamic properties of Au(HS)<sub>2</sub><sup>-</sup> (ref. 8). Fluorescence spectra recorded on these solutions are in perfect agreement with the dominant presence of this complex in which Au is linearly coordinated with 2±0.2 sulfur atoms at 2.29±0.01 Å over the wide temperature range (Fig. C & D).

A very similar Au 1<sup>st</sup> shell environment is found in S-H<sub>2</sub>O fluids (N<sub>Au-S</sub>=2.2±0.3, R<sub>Au-S</sub>=2.29 Å at 300 and 400°C, experiment 7). However, some subtle differences in the 2<sup>nd</sup> shell are detected (Fig. D). The derived structural parameters are inconsistent with the neutral mono-sulfide complex AuSH<sup>0</sup> which has been widely believed the dominant Au species in S-bearing acid solutions<sup>8</sup>. Moreover, the measured Au solubilities are 1 to 2 orders of magnitude higher than those predicted using the AuSH<sup>0</sup> thermodynamic properties (Fig. B). These findings strongly

suggest that Au is likely to be complexed with other sulfur ligands like  $\text{SO}_2$  in these acid solutions by forming species with linear S-Au-S arrangement like  $\text{Au}(\text{SO}_3)_2^{3-}$ , similar to the well-known thiosulfate  $\text{Au}(\text{S}_2\text{O}_3)_2^{3-}$  complex stable at low temperatures<sup>9</sup>. This unexpected result may have important implications for Au transport by high-temperature magmatic fluids (> 450-500°C) in which  $\text{SO}_2$  largely dominates over  $\text{H}_2\text{S}$ .

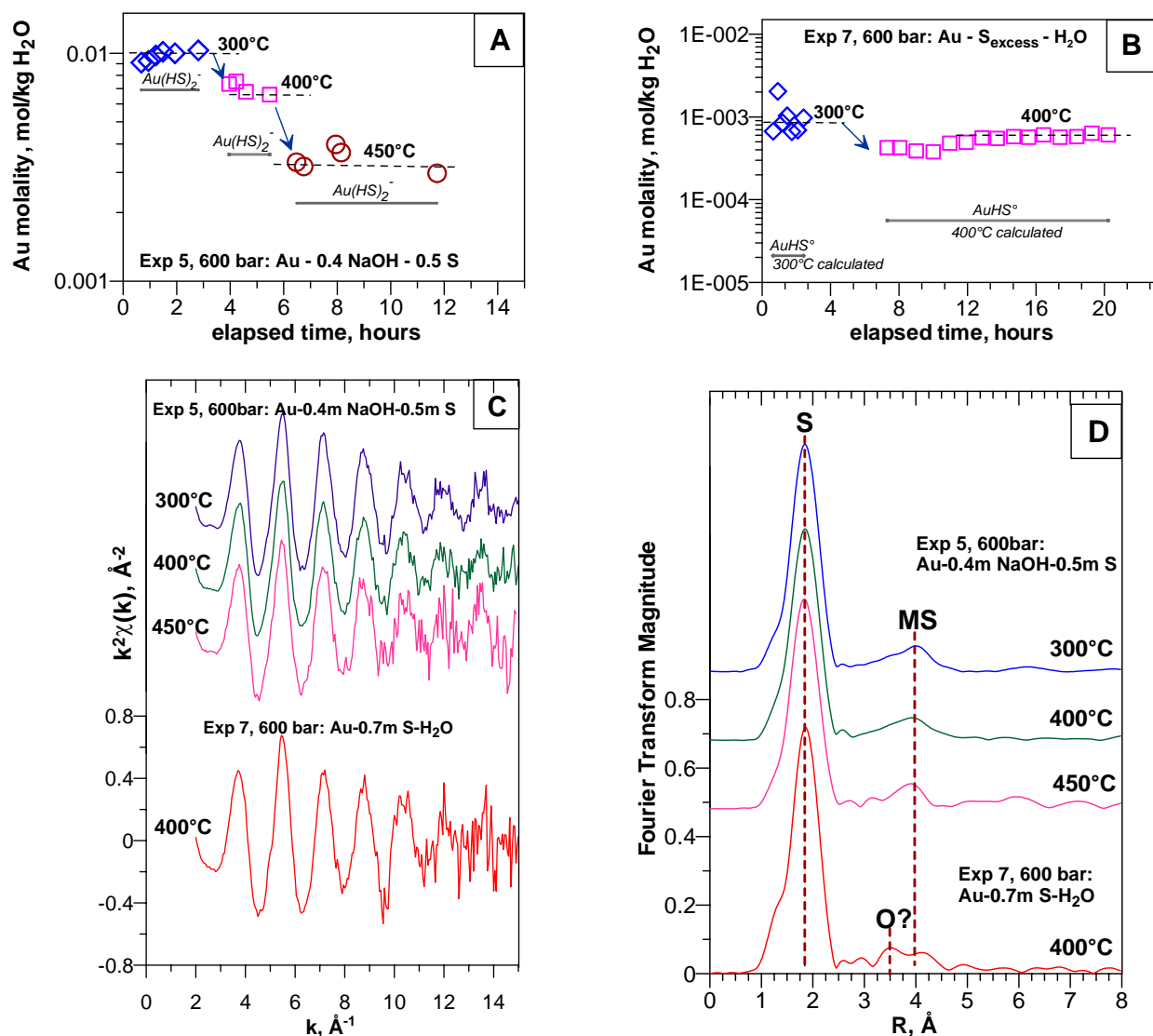


**Fig. A & B.** Gold concentrations derived from absorption-edge height in transmission mode as a function of time and temperature in two XAFS experiments. Each symbol corresponds to a XAFS scan; arrows indicate temperature changes during the run. Horizontal grey bars denote calculated Au concentrations at each temperature using the thermodynamic properties of the major  $\text{AuHS}$  and  $\text{Au}(\text{HS})_2^-$  complexes and sulfur species. Uncertainties associated with these calculations are at least  $\pm 0.3$  log units.

**Fig. C & D.** Typical fluorescence EXAFS spectra and their corresponding FT's at indicated conditions. Note a good quality of the spectra to at least  $10\text{-}12 \text{ \AA}^{-1}$ . MS denote multiple scattering within the linear S-Au-S cluster.

**Conclusions & perspectives.** To our knowledge, this experiment is the first quantitative measurement of gold solubility and structure of Au-sulfide species at hydrothermal conditions using *in situ* XAFS spectroscopy. At near-neutral to basic pH, our data are in excellent agreement with numerous batch-reactor solubility studies and are fully consistent with the dominant formation of the  $\text{Au}(\text{SH})_2^-$  complex at least between 200 and 450°C. At acid pH, however, our results indicate the formation of new species presumably with sulfite ( $\text{SO}_2$ ). Considering both the poorly quantified chemical speciation and low kinetics of sulfur equilibration in acid solution, more measurements on Au and its analogs (Ag, Cu) by XAFS/batch-reactor, and sulfur species by Raman spectroscopy will be performed in these systems.

### References

1. Testemale D. et al. (2005) Rev. Sci. Instrum. 76, 43905;
2. Pokrovski G.S. et al. (2005) Chem. Geology 217, 127;
3. Pokrovski G.S. et al. (2005) GCA 69, A734;
4. Berrodier I. et al. (2004) GCA 68, 3019;
5. Murphy P.J. et al. (2000) GCA 64, 479;
6. Gammons C.H. & Willams-Jones A.E. (1997) GCA 61, 1971;
7. SUPCRT 96;
8. Tagirov B.R. et al. (2005) GCA 69, 2119;
9. Bryce R.A. et al. (2003) J. Phys. Chem. A 107, 2516.